

## Numerical simulation temperature field of laser cladding titanium alloy

Guang Yang<sup>1,a</sup>, Wei Wang<sup>1,b</sup>, Lanyun Qin<sup>1,2,c</sup>, Xingliang Wang<sup>1,d</sup>

<sup>1</sup>School of Mechanical Engineering, Shenyang Aerospace University, Shenyang, 110134, China

<sup>2</sup>School of Mechanical Engineering, Shenyang University of Technology, Shenyang, 110016, China

<sup>a</sup>yangguang@sau.edu.cn, <sup>b</sup>wangwei1116@sau.edu.cn

<sup>c</sup>qinly@sau.edu.cn, <sup>d</sup>rpm@sau.edu.cn

**Key words:** laser meter deposition shaping; numerical simulation; transient temperature field; temperature gradient

**Abstract:** In order to control the thermal stress of cladding, a numerical simulation of temperature field during multi-track & multi-layer laser metal deposition (LMD) process is developed with ABAQUS based on “element birth and death” technology of FEM. The dynamic variances of temperature field and stress field of forming process are calculated with the energy compensation of interaction between molten pool-powder. The temperature field, temperature gradient, thermal stress field and distribution of residual stress are obtained. The results indicate that although the nodes on different layers are activated at different time, their temperature variations are similar. The temperature gradients of samples are larger near the molten pool area and mainly along z-direction.

### Introduction

As a good mechanical properties of the metal Titanium alloy has been applied in many fields. But its application in friction parts is much be limited for its poor wear ability. In order to expand the application range of titanium alloy, the scientists have been working to improve its wear resistance. Laser cladding is a new type of surface modification technology, which can greatly improve the material surface properties through the rapid solidification process [1]. This article chooses Ti and Cr<sub>3</sub>C<sub>2</sub> for cladding layer material to fabricate TiC reinforced wear-resisting coating.

Because of higher power, rapid heating and cooling rate, small size molten pool, high temperature in laser cladding, it is very difficult to measure its internal temperature distribution and the cooling speed. At present, material temperature field distribution under the action of laser is obtained by means of numerical analysis and numerical simulation[2]. The domestic scholar have been doing lot of research on the temperature field and stress field of laser cladding[3-6].

To analyze the major factors that affect temperature field during the laser cladding, the paper builds a finite element model of temperature field of titanium alloys laser cladding in consideration of heat source model, material thermal physical property and meshing situation. Then the calculation result is analysed to optimize titanium alloy laser cladding process parameters.

### Mathematical model and boundary condition

**Mathematical model:** In the sight of basic principle on conductions of heat, Fourier heat conduction differential equation(Eq. 1) of temperature field is founded for laser cladding 3D transient temperature field heat source.

$$\rho C_p \frac{\partial T}{\partial t} = \nabla \cdot (k \nabla T) + \bar{Q} \quad (1)$$

Where  $\rho$  is the density ( $kg/m^3$ ),  $C_p$  is specific heat ( $J/kg, K$ );  $k$  for the coefficient of thermal conductivity ( $W/(m, K)$ );  $\bar{Q}$  for internal heat source intensity;  $T$  for temperature,  $t$  for time, of which  $C_p$ ,  $k$  are changing with temperature. Initial conditions: when  $t = 0$ , the work piece is uniform initial temperature and it is commonly ambient temperature.

Thermal boundary conditions: during the laser cladding, surface heat loss for work piece is mainly caused by radiation and the thermal convection. To simplify the calculation, only convective and

radioactive components were considered to transfer heat to surrounding media during the simulation, i.e. the third class boundary conditions was imposed on matrix and the cladding layer surface. The ambient temperature and convection coefficient between matrix and air were held constant, where the environmental temperature were set to 293K and convection coefficient between matrix and air were set to  $10\text{W}/(\text{m}^2\cdot\text{K})$  to meet equation (2). In order to reflect relationship of the heat transfer and temperature more accurately, heat transfer coefficient could be appropriately increase for some high temperature surface.

$$(a_c + a_r)(T - T_0) = -k \frac{\partial T}{\partial n} \quad (2)$$

**The model of laser heat source:** Body heat source model are usually adopted during the numerical simulation of laser welding. Heat energy is transferred to specimen via the definite action area named heating up spot during laser machining. Heat distribution of the spot is not uniformly, there is much heat at the center but little at the fringe. As shown in figure 1 Friedman described the distributing of heat flux density on the heating up spot by Gauss model. The density of heat flux of a random point A around the heating center can be formulated as equation 3.

$$q(r) = q_m \exp\left(-\frac{3r^2}{R^2}\right) \quad (3)$$

Where  $q_m$  is maximum heat flux density at the heating up spot center, R is laser effective heated radius, r is the distance from point A to the heating up spot center.

This heat source model is widely applied in calculating laser machining temperature field using finite element methods. A relatively exact result can be got by this model in the case that the wallop of the laser heat source to the molten pool is small.

So laser heating is simulated by Gauss heat source, then the heat source can be controlled to move by user subroutine of finite element (FE) software and it can provide corresponding density of heat flux at different moment and different position.

**Material thermo-physical properties:** The experimental substrate is TC4 titanium alloy, which nominal thermo-physical properties is shown in Tab.1, and the cladding layer powder material is mixtures of  $\text{Cr}_3\text{C}_2$  powder and pure Ti powder. The thermo-physical properties of  $\text{Cr}_3\text{C}_2$  and Ti powder are shown in Tab.2 and Tab.3. As the thermo-physical properties of material are of great influence on calculating temperature field, which directly affect the shape and size of the laser cladding temperature field, it is necessary to take into account temperature dependency of the thermal properties of the material

Table 1 Thermo-physical properties of TC4 titanium alloy

melting points[°C]: 1540~1650 density[kg/m³]: 4440											
T[°C]	20	100	200	300	400	500	600	800	1000	1400	1600
heat conductivity[W/(m·°C)]	6.8	7.4	8.7	9.8	10.3	11.8	12.4	14.4	15.8	24.3	22.2
Specific heat[J/(kg·°C)]	611	624	653	674	691	703	708	727	751	783	898
Coefficient of linear expansion[10 <sup>-6</sup> /K]	9.0	9.0	9.0	9.0	9.0	9.4	9.4	9.7	9.7	9.7	9.7

Table 2 Thermo-physical properties of  $\text{Cr}_3\text{C}_2$

specific heat [kJ/kg·K]	coefficient of linear expansion[10 <sup>-6</sup> /K]	elastic modulus[Pa]	density [kg/m³]	Melting points [°C]	heat conductivity [W/m·K]
0.3	6.74	0.355E11	6900	3530	19

Table 3 Thermo-physical properties of titanium

melting points[°C]: 1668±4 density:[kg/m³]: 4540											
T[°C]	100	200	300	400	500	600	700	800	900	1000	
heat conductivity[W/(m·°C)]	20.7	19.9	19.5	19.4	19.4	19.9	—	—	—	—	
specific heat[J/(kg·°C)]	469	481	510	536	569	—	—	—	—	—	
Coefficient of expansion [10 <sup>-6</sup> /K]	11.1	12.1	12.8	13.4	13.9	14.4	14.8	12.9	12.5	13.1	

**Model and mesh:** The computational models are about substrate and cladding layer, of which size of substrate is  $30 \times 30 \times 5\text{mm}$ , and the model of cladding layer is divided into four passes and its size is  $20 \times 7.66 \times 0.5\text{mm}$ . As laser cladding is a process in which temperature changes rapidly along with time

and space and the temperature gradient is great, the mesh in the laser scanning area and near it should be divided precisely and the other area could be divided roughly. For three-dimensional problem, ABAQUS thermal simulation adopt DC3D8 cell, and its minimum step of time is controlled in 0.01s. The model and finite element mesh are shown in figure 2.

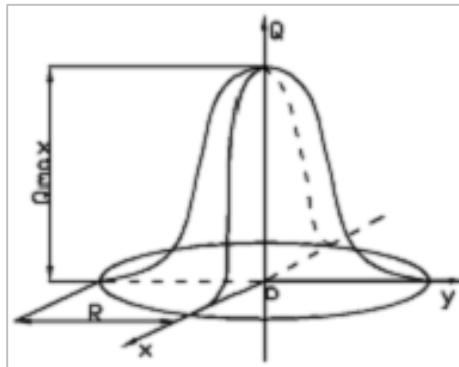


Fig.1 Sketch of Gauss Heat Source

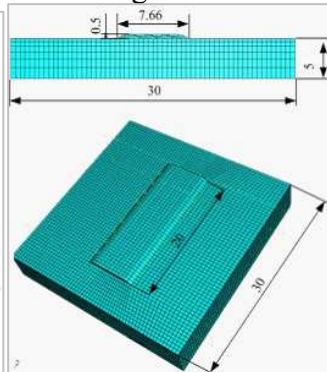


Fig.2 Sketch mesh of coating and substrate

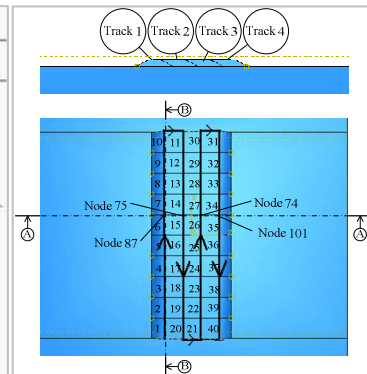


Fig.3 Each element group sediments and main node location

**Model of finite element method:** The locations for main node and each element group sediments are shown in figure 3. The coating is divided into four passes and each contains 10 element groups, which means there are 40 element groups altogether. The laser use snake-like scanning mode, and all cladding layers element group are deactivated before simulation. The element group which is in the scope of laser beam will be activated in every calculation step.

**Assumptions:** To simplify calculation the follow assumptions is made:

- 1) Materials are isotropic;
- 2) Neglecting the flow function of molten pool fluid;
- 3) Neglecting material vaporization ;
- 4) Neglecting keyholes effects, latent heat of phase change and thermal deformation.

## Results and discussion

**The influence of the laser power:** In the process of FEM the laser power is 1000W, 1500W and 1800W respectively and the scanning speed is 5mm/s, the beam spot diameter is 2.5mm.

Figure 4 shows temperature field distribution at different power in 2.1s. It can be found that the laser power has made the significant influence on the highest temperature of molten pool, the highest temperature is rising with the enhance of laser power, but the trend of temperature field distribution is roughly the same. When laser power is 1000W, 1500W, 1800W, the corresponding highest temperature is 1679°C, 2260°C, 2638°C. Then it can be summed up that the highest temperature of molten pool at 1800w is 959°C higher than that at 1000W. At the same time, with the enhance of laser power, the temperature gradient, the breadth and depth of molten pool are both increased considerably.

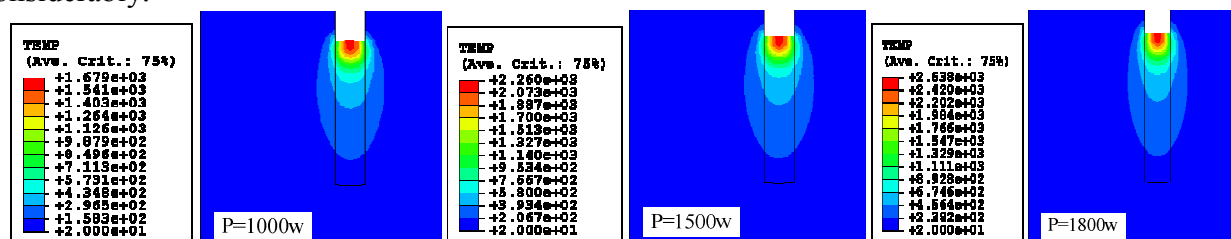


Fig.4 Temperature field distributions at different laser power

The nodes thermal cycling curve under 1000W、1500W、1800W laser power is shown figure 5. It can be seen that the thermal cycling curve under different laser power appear to be very similar in shape, the temperature of node 87 (As shown in the Fig. 3) reach maximum in 2.4s under different laser power. Retention time of high temperature is much longer when laser power increases for higher

laser power means more energy output and absorption. It still can be obtained from figure 5 that node 87 can be heated again when laser scans to node 75, 74 and its temperature also can reach to 500°C around, which means the coating will be heated again. It can be found that the molten pool highest temperature will rise with the process of titanium alloy laser powder deposition forming through observing the highest temperature of nodes 87, 75, 74, 101 in figure. When the laser power is 1800W, the node 101 temperature is 2956 °C, which is 318 °C higher than node 87 whose temperature is 2638 °C.

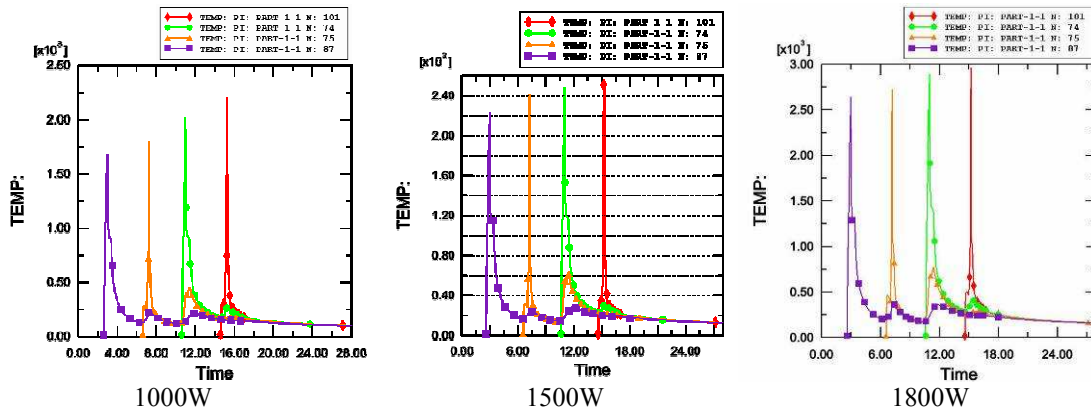


Fig.5 Different nodes thermal cycling curve under different laser power

**Influence of the laser scanning speed:** During the simulation process, the laser power is 1500W, the scanning speed is 4mm/s, 5mm/s and 10mm/s, and the spot diameter is 2.5mm.

Figure 6 is the temperature distribution map of the first pass B-B section when scanning speed is 4mm/s, 5mm/s and 10mm/s. figure 7 is the map of A-A section. Figure 8 is temperature cycling curve of node 87 at different scanning speed.

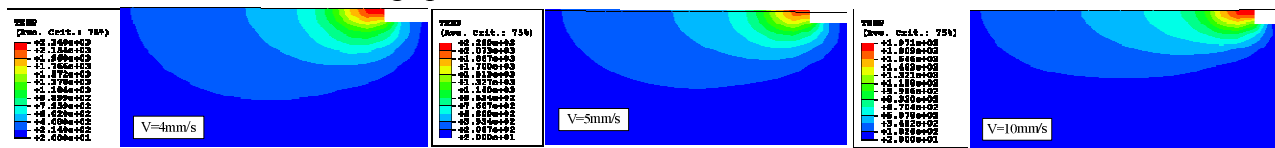


Fig.6 Temperature field of flare center through the first line(B-B) at different laser scanning speed

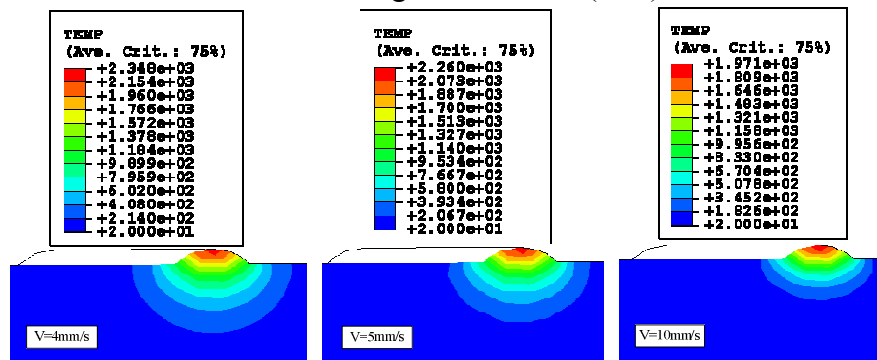


Fig7 Temperature field distribution map at different laser scanning speed

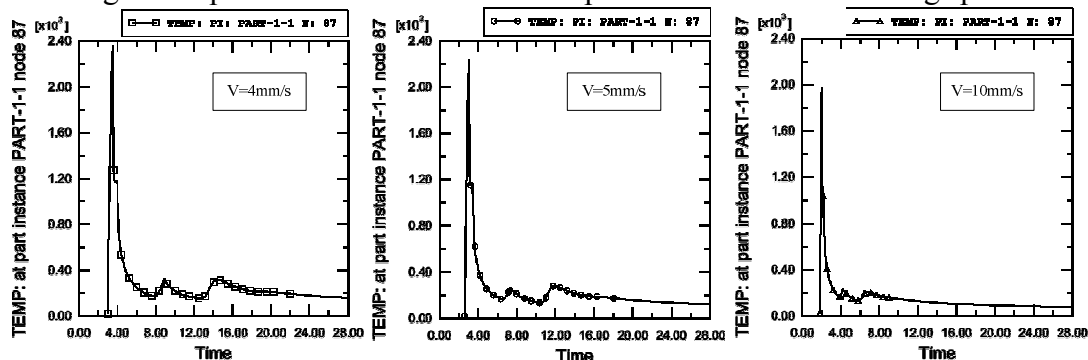


Fig8 Temperature cycling curve of node 87 by different laser scanning speed

It can be seen from the temperature distribution that the larger scanning speed is, the lower highest temperature in the section and the smaller width and depth of molten pool is. And also the maximum and minimum temperature is declining. The highest temperature declines from 2348°C to 1971°C when the scanning speed rises from 4mm/s to 10mm/s. That is for the faster laser scanning speed is, the shorter time laser heated on each tiny unit on the model time. Fig. 6 indicates that temperature gradient is also falling with the increase of laser scanning speed. It can be seen from Fig.7 that heat affected zone decreases obviously with the laser scanning speed increase for short acting time.

Temperature cycling curve indicates that with laser scanning speed increase peak temperature of a point on the first pass of deposition declined, at the same time the reach time became short. For example, node 87 reached its peak temperature in 3.5s at 4mm/s scanning speed, while the reach time is 2s at 4mm/s scanning speed. Along with the increase of the scanning speed, temperature peak width became narrow for short high temperature residence time. It is also can be seen from Fig.8 the node 87 would be heated again when laser scanned node 75 and node 74 (As shown in the Fig. 3), and its temperature rose to about 400°C. That is the deposited pass would be heated again, and the time reaching peak temperature became short with the increasement of scanning speed.

## Conclusion

1) Increasing the laser power lead to overall temperature and temperature gradient risen. So the laser power should be decreased in the guarantee of the powder well melting and forming good metallurgical combination between coating and substrate.

2) The temperature gradient would be risen with the increasement of the scanning speed. The appropriate scanning speed should be applied to keep laser machining efficiency and the size of heat affected zone.

3) For the preheat action of multi pass lap, the temperature of cladding layer node will gradually elevate to peak temperature in the order of cladding and the rising trend is similar. Meanwhile that temperature of every cladding layer every node can exceed the powder melting point to forming the cladding layer.

## References

- [1] Ma Lin, Yuan Jin-ping, Zhang Ping, et al. Transactions of the China Welding Institution, 2007, 28 (7): 110-112. (In Chinese)
- [2] Zeng Da-wen, Xie Changsheng. Materials Science & Engineering, 1997, 15(4): 1-9 (In Chinese)
- [3] Hao Nanhai, Lu Wei. China Surface Engineering, 2005, 1(70) : 20-23. (In Chinese)
- [4] Liu Zhenfeng. 3D FEM numerical simulation on the temperature field of laser cladding by powder injection [D]. Wuhan: Huazhong University of Science & Technology. 2006. (In Chinese)
- [5] Zhao Hongyun, Shu Fengyuan, Zhong Hongtao et al. Transactions of the China Welding Institution, 2010, 31(5): 82-84. (In Chinese)
- [6] Xue Chunfang, Dai Yao, Wang Danjie, et al. Journal of Academy of Armored Force Engineering, 2006, 20 (3) : 94-96. (In Chinese)
- [7] Chen Bingsen. Welding technology of computer aided [M]. Beijing: China Machine Press, 1999, 166-178. (In Chinese)
- [8] Goldak John, Chakravarti Aditya, Bibby Malcolm.. Metallurgical Transactions B (Process Metallurgy), 1984, 15B(2): 299-305.
- [9] Chang W S, Na S J. Journal of Materials Processing Technology, 2002, 120(1/3): 208-214.
- [10] Carmignani C, Mares R, Toselli G. Computer Methods in Applied Mechanics and Engineering, 1999, 179(3): 197-212.
- [11] Shang Xiaofeng. Research on metal powder laser shaping [D]. Shenyang: Shenyang Institute of Automation Chinese Academy of Sciences, 2005. (In Chinese)

## **Materials and Computational Mechanics**

10.4028/www.scientific.net/AMM.117-119

## **Numerical Simulation Temperature Field of Laser Cladding Titanium Alloy**

10.4028/www.scientific.net/AMM.117-119.1633